

Acid and base recovery from brine solution using PVP intermediate-based bipolar membrane through water splitting technology

Krishnaveni Venugopal¹ · Minnoli Murugappan¹ · Sangeetha Dharmalingam¹

Received: 20 March 2015 / Accepted: 25 September 2015 / Published online: 27 October 2015
© The Author(s) 2015. This article is published with open access at Springerlink.com

Abstract Potable water has become a scarce resource in many countries. In fact, the world is not running out of water, but rather, the relatively fixed quantity is becoming too contaminated for many applications. Hence, the present work was designed to evaluate the desalination efficiency of resin and glass fiber-reinforced Polysulfone polymer-based monopolar and bipolar (BPM) ion exchange membranes (with polyvinyl pyrrolidone as the intermediate layer) on a real sample brine solution for 8 h duration. The prepared ion exchange membranes (IEMs) were characterized using FTIR, SEM, TGA, water absorption, and contact angle measurements. The BPM efficiency, electrical conductivity, salinity, sodium, and chloride ion concentration were evaluated for both prepared and commercial-based IEM systems. The current efficiency and energy consumption values obtained during BPMED process were found to be 45 % and 0.41 Wh for RPSu-PVP-based IEM system and 38 % and 1.60 Wh for PSDVB-based IEM system, respectively.

Keywords Brine water desalination · Reinforced IEM · PVP intermediate based BPM · Water dissociation reaction · BPM efficiency

Introduction

Potable water has become a scarce resource in many countries, developed and developing alike. In India, there are many villages and towns which do not have adequate and reliable sources of drinking water of required qualities. This is mainly due to factors like saline underground water, contaminated water absolutely unfit for human consumption, dug up wells that yield water of poor quality, and dry up in summer. No source attracts such special attention as the problem of water supply in the current scenario. Hence it becomes essential to find a source for drinking water from other water bodies such as brackish water, sea water, sewage water etc., using suitable techniques. Desalination is one such technique, with its various categories it could be effectively used for water purification. Among the various categories, membrane-based technology is the most popular method for its wide application.

Membranes especially a class of ion exchange membranes (IEMs) is one of the advanced technological products mainly used for various industrial applications such as potable water production from the sea through reverse osmosis, recovery of valuable constituents from industrial effluents through the electrolysis process (Volkov et al. 2008; Ostwald 1890) etc. Recently, a special kind of IEM called as bipolar membranes (BPMs) or catalytic membranes have been developed for electro-membrane processes to split water into protons and hydroxyl ions (Kressman and Tye 1956; Friette 1956). From the literature survey, it was identified that to meet the growing requirements of science and technology, several attempts were made to modify the existing IEMs. And surface modification of the membranes was observed as one of the ways that could be employed to minimize the undesired properties and also to introduce the additional functional

✉ Sangeetha Dharmalingam
sangeetha@annauniv.edu

¹ Department of Mechanical Engineering, Anna University, Guindy, Chennai, Tamil Nadu 600025, India

properties for a polymer separation membrane (Ulbricht 2006).

On similar lines, the work in the present study was designed to evaluate the desalination efficiency of resin and glass fiber-reinforced Polysulfone (PSu) polymer-based monopolar (cation exchange and anion exchange) and bipolar [with polyvinyl pyrrolidone (PVP) as the intermediate layer (IL)] ion exchange membranes in terms of various process parameters on a real sample brine solution containing 10,000 ppm up to 8 h. The prepared IEMs were characterized using FTIR, SEM, TGA, contact angle measurements, and laboratory technique. In addition, the water dissociation capacity of the prepared BPM with PVP intermediates was tested in a two compartment electrodiolytic cell that was fabricated in laboratory scale. The experimental results were compared with the results obtained by using commercially available polystyrene divinylbenzene-based (PSDVB) membranes under similar experimental conditions. In addition, for all the obtained final feed solutions after the performance, sodium-chloride ion concentration, salinity, and electrical conductivity of ions were determined.

Materials and methods

Preparation of reinforced IEMs

Anionic and cationic functionalized PSu-based ionomers (i.e., QPSu and SPSu ionomers) were obtained as reported earlier (Krishnaveni and Sangeetha 2012). To introduce additional functional properties like higher ion exchange capacity (IEC) with firmness and strength for a polymer separation membrane, reinforced CEM (RCEM) i.e., reinforced sulfonated Polysulfone (RSPSu) and reinforced AEM (RAEM) i.e., reinforced quaternized Polysulfone (RQPSu) were prepared with resin and glass fiber reinforcement in the synthesized cationic and anionic ionomers. Weighed amount of ion exchange resin (IER) was dried in an oven at 60 °C for 24 h before use. RCEM/RAEM based on PSu polymer was prepared by first dispersing a specific quantity (from 10 to 70 %) of dried (60 °C for 24 h in an oven) and crushed CER/AER in either SPSu-N, *N*'-dimethylformamide (DMF), or QPSu-DMF solution respectively for 12 h using a magnetic stirrer at room temperature. In order to break the aggregates and to obtain a uniform dispersion, the solution was sonicated for 30 min. Then, the solution was cast on a clean glass petri dish and the glass fiber matrix was placed to get immersed in the solution before drying in the oven for 24 h at 80 °C. The conductivity for the obtained membranes with various resin contents was determined using impe-

dance spectroscopy. For this, the membranes with required dimensions were cut and pretreated with 0.01 N sulfuric acid and kept in water for 100 % hydration. From the difference between the resistance of the blank cell and the one with a membrane separating the working and counter electrode compartments, the resistance of the membrane was calculated and then it was converted to their conductivity values. From the results (Krishnaveni and Sangeetha 2015) it was confirmed that the conductivity of the prepared membranes, increased with increase in IER loading below 50 %, beyond which the membranes became brittle (Kumar and Shahi 2010). Hence, the resin loading was optimized at 40 % for both resins.

The prepared RCEM and RAEM from PSu polymer were cut into pieces of 10 cm × 12 cm size and pretreated using 1 M NaOH and 1 M HCl solutions then finally equilibrated with 2 M NaCl solution, washed with distilled water, and dried. Now these both layers act as cationic exchange layer (CEL) and anionic exchange layer (AEL) for the reinforced BPM (RBPM). Then on one side of both CEL and AEL layers, a solution containing approximately 0.12 g of PVP-based conducting polymer in 6 mL of ethanol solvent was coated to form the IL. Finally the IL-coated sides of both layers (CEL and AEL) were sandwiched and subjected to hot press for 5 min at a temperature and pressure of about 90 °C and 3 ton, respectively, and the finally obtained RBPM is now represented as RBPM-PVP.

Reinforced IEM characterization

The resin incorporation into functionalized membranes was confirmed with Perkin Elmer RX I FTIR spectrophotometer. The thermal stability of the prepared membranes was studied using SDT Q 600 US analyzer (ASTM E1131) under a nitrogen atmosphere at a heating rate of 20 °C min⁻¹ from RT to 700 °C. The surface morphology of the membranes was obtained using field emission HITACHI S-3400 SEM instrument. The hydrophilic and hydrophobic nature of the membrane was studied using Goniometer-sessile drop meter GBX-Digi-drop wetting and spreading studies. The conductivity of the membrane was determined using impedance spectroscopy. The characterization studies such as water absorption and IEC for the prepared membranes were measured using the similar procedure as discussed earlier (Krishnaveni and Sangeetha 2012). The chemical stability of the membranes was determined by accelerating the degradation process in the membranes using a solution containing 4 ppm of ammonium iron (II) sulfate hexahydrate and 15 ml of H₂O₂ (3 %) (Fenton's reagent) in 500 ml distilled water at 60 °C for about an hour.

Electrodialytic IEM stack for brine desalination

The fabricated bipolar membrane electro dialysis (BPMED) unit and the commercial PSDVB-based BPM used in the study were supplied by Arun Electrochemical, Chennai. The description of the instrument used for determination of both BPM efficiency and brine desalination is laboratory scale fabricated two compartments and five compartments electro dialytic cells. The volume of each chamber was about 160 cm^3 and was connected to a tank of 1 L capacity of the distilled water solution, allowing for batch mode recirculation of external solutions by submersible pumps. The effective membrane areas of each IEM are about 120 cm^2 . The configuration of the membrane arrangement in the five compartments stack was in the order BP–A–C–BP in between the electrodes. The cathode and anode electrodes used were stainless steel and Ti coated with Ti–Ru–Pd oxides, respectively. The two electrodes were connected to a DC power supply. The two electrolyte compartments (EC) were on both the extremes adjacent to electrodes, two concentrated compartments [acid compartment (AC) and base compartment (BC)] adjacent to the central compartment on either side where acid and base were collected, and one dilute central feed compartment (FC) where sample to be treated are taken. The commercial monopolar membranes (CMI-7000S and AMI-7001S) used for comparison was purchased from International INC, New Jersey, USA.

In order to minimize the cell voltage generated during the initial stages of the experiments, dilute HCl (0.01 N) and dilute NaOH (0.01 N) solutions were used in AC and BC, respectively. And 0.05 mol L^{-1} of NaCl solution was taken in each EC. The experiments were carried out at the initial voltage of 10 V. During the performance, at every 15 min time interval, process parameters such as membrane stack potential, pH (in AC, BC, EC, and FC), and acid–base concentration of the solutions (in AC and BC) were determined by means of digital multimeters, pH meter (Hanna HI 96107 pocket size pH meter), and standard acid–base titration procedure, respectively. In addition, other parameters such as energy consumption, current efficiency (CE), Transport number (T. No.) of ions, water dissociation efficiency (WDE), and water dissociation flux were determined using the same set of equations as reported earlier (Krishnaveni and Sangeetha 2014a, b). Finally, after 8 h treatment, the feed sample was analyzed for their salinity and electrical conductivity using WTW LF 197-S EC meter. The chloride ion and sodium ion concentrations in these samples were measured by argentometric method and flame photometry, respectively.

Results and discussion

FTIR characterization

Pristine Polysulfone (PSu), RCEM (i.e., RSPSu) and RAEM (i.e., RQPSu) membrane samples were characterized using FTIR (Fig. 1) to confirm their structure and reinforced resin incorporation. The appearance of bands at 3026 and 756 cm^{-1} in Fig. 2a was due to the ν_s (C–H) and δ (C–H) vibration bond of aromatic hydrocarbons, respectively. Appearance of bands at 1411 and 1387 cm^{-1} was due to the aliphatic ν_{as} (C–H) and ν_s (C–H) vibration, respectively. A doublet peak at 1589 cm^{-1} was due to Aromatic ν_s (C=C) vibration. The peaks at 1163 and 1320 cm^{-1} were due to the ν_s (SO₂) and ν_{as} (SO₂) group vibration, respectively. The peak at 692 cm^{-1} was due to ν (C–S) vibration and peak at 1113 and 1298 cm^{-1} represents ν_s (C–O–C) and ν_{as} (C–O–C) vibrations, respectively. The appearance of all these peaks confirmed the structure of PSu. The appearance of a broad and intense envelope around 3447 cm^{-1} (Fig. 1b) was attributed to -OH stretch of the sulfonic acid group (present in both resin and membrane matrix) while the peak around 1161 cm^{-1} was due to the O=S=O (asymmetric stretch) group and this confirmed the sulfonation of PSu. The appearance of a peak at around 854 cm^{-1} suggested that the sulfonic acid group was substituted at the para position. The broad peak at 3392 cm^{-1} in Fig. 1c was assigned to the characteristic peak of ν_{as} (NR₃⁺). Appearance of peak around 1320 cm^{-1} was due to C–N stretching, vibration, and this confirmed the presence of amine group in the membrane matrix. From the peak intensity obtained, it was clear that resin

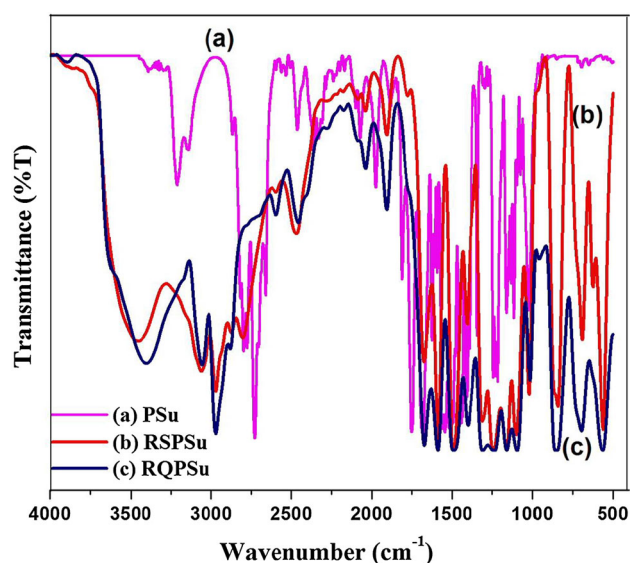


Fig. 1 FTIR spectra of a PSu, b RSPSu, and c RQPSu membranes

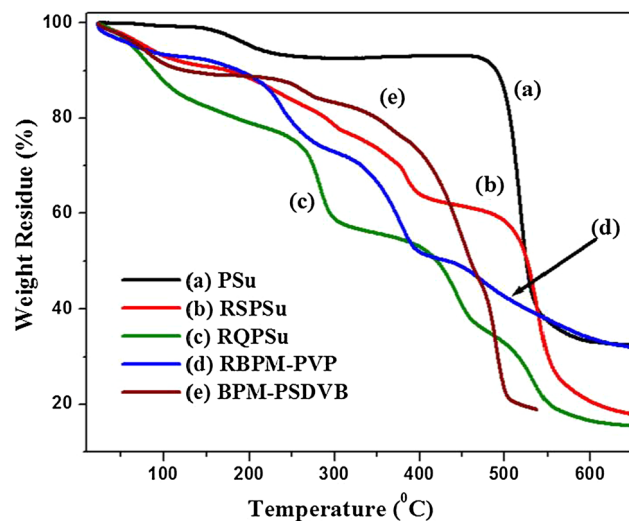


Fig. 2 TGA curves of *a* PSu, *b* RSPSu, *c* RQPSu, *d* RBPM-PVP, and *e* BPM-PSDVB membranes

incorporation, in addition to quaternization and sulfonation reactions, resulted in an increase in the number of ion exchange groups in the membrane.

Thermogravimetric analysis

The TGA curves for the reinforced monopolar and BPM are shown in Fig. 2. The reasons for the observed various degradation steps at different temperatures for both commercial and synthesized IEM are given in Table 1. The TGA curve of pristine PSu as observed in Fig. 2a, exhibits two stage degradation. The first step indicated the loss of bound water and traces of solvent up to 270 °C and beyond which no further weight loss was observed until 476 °C. The steep loss in weight observed beyond 490 °C was indicative of the polymer degradation.

SEM analysis

The SEM images of various IEMs such as RSPSu, RQPSu, and RBPM-PVP are shown in Fig. 3. The uniform distribution of resin particles throughout the reinforced membrane surface was observed for RSPSu and RQPSu membranes. On the other hand, cross-sectional view of reinforced PSu-PVP-based BPM clearly showed three distinct regions. The top layer was an anion exchange layer (AEL) or QPSu while the thin middle one represented the PVP-IL. The last layer (third layer) corresponded to cation exchange layer (CEL) or SPSu. The appearance of small spheres on both top and bottom surfaces of an RBPM-PVP represents the IER particles.

Contact angle measurement

From Fig. 4 on comparisons between the average contact angle of pristine (82.51°), PVP-coated membranes (50.25°) and reinforced functionalized membranes, it was identified that the introduction of functional group converted hydrophobic nature of the base polymer (pristine) into hydrophilic nature with a small contact angle measurement value as studied by Dias and de Pinho (1999) and Guan et al. (2005). Also, the contact angles for the commercial monopolar membranes such as CEM-PSDVB and AEM-PSDVB were measured to be 86.70° and 93.09°, respectively. A contact angle value for the reinforced functionalized membranes such as RSPSu and RQPSu could not be measured because of the complete absorption of water. This infers the increased hydrophilicity of these membranes than the pristine membrane due to the presence of functional groups, resin, and fiber reinforcements (Sachdeva et al. 2008). In order to determine the nature of PVP intermediate in a BPM, one face of the membrane was coated with PVP solution and its contact angle was measured.

Table 1 Representation of degradation temperature and its reason for various IEMs

Reason for degradation	Membrane code with degradation temperature			
	RSPSu (3 steps as from Fig. 2b)	RQPSu (3 steps as from Fig. 2c)	RBPM-PVP (4 steps as from Fig. 2d)	PSDVB (3 steps as from Fig. 2e)
Removal of physically and chemically bonded water + trace amount of solvent	Up to 152 °C	Up to 137 °C	Up to 131 °C	Up to 129 °C
Degradation of functional groups (either sulfonic acid and/or quaternary ammonium group) from the polymer chain	Between 366 and 438 °C (–SO ₃ H)	Between 266 and 404 °C (–NR ₃ ⁺)	Between 202 and 309 °C (both)	Between 249 and 311 °C (both)
Degradation of intermediate molecule from the membrane	–	–	Between 334 and 453 °C (–NR ₃ ⁺)	–
Removal of loosely bound resin particles on surface and from polymer matrix	–	–	–	–
Removal of reinforced fiber from the polymer matrix	Between 504 and 578 °C	Beyond 529 °C	Beyond 456 °C	Beyond 336 °C
Polymer main chain degradation	–	–	–	–

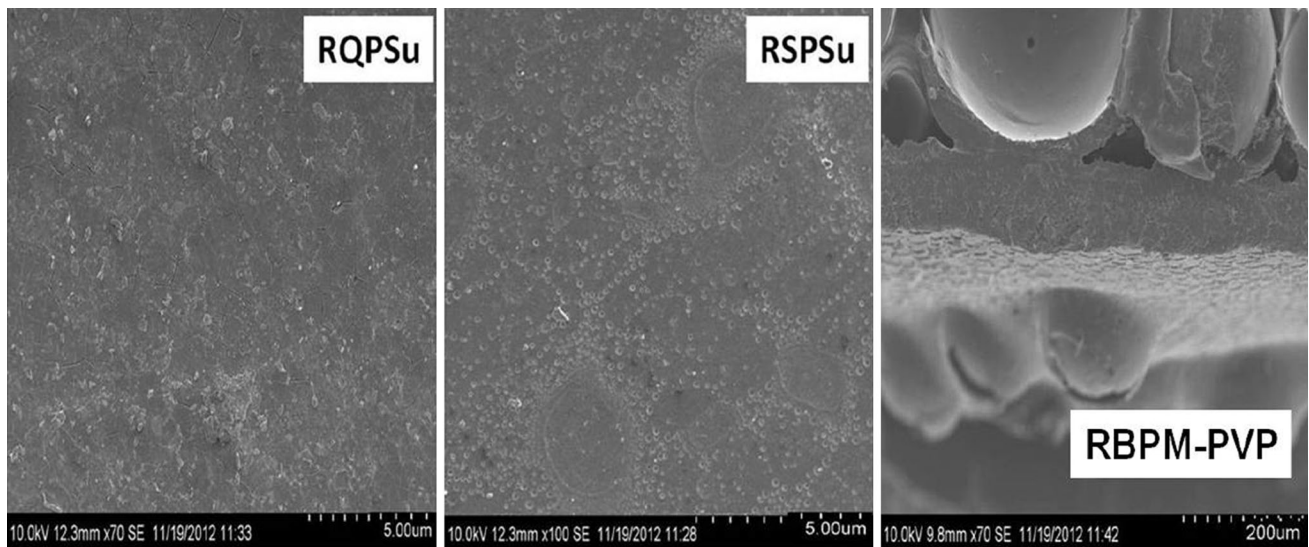
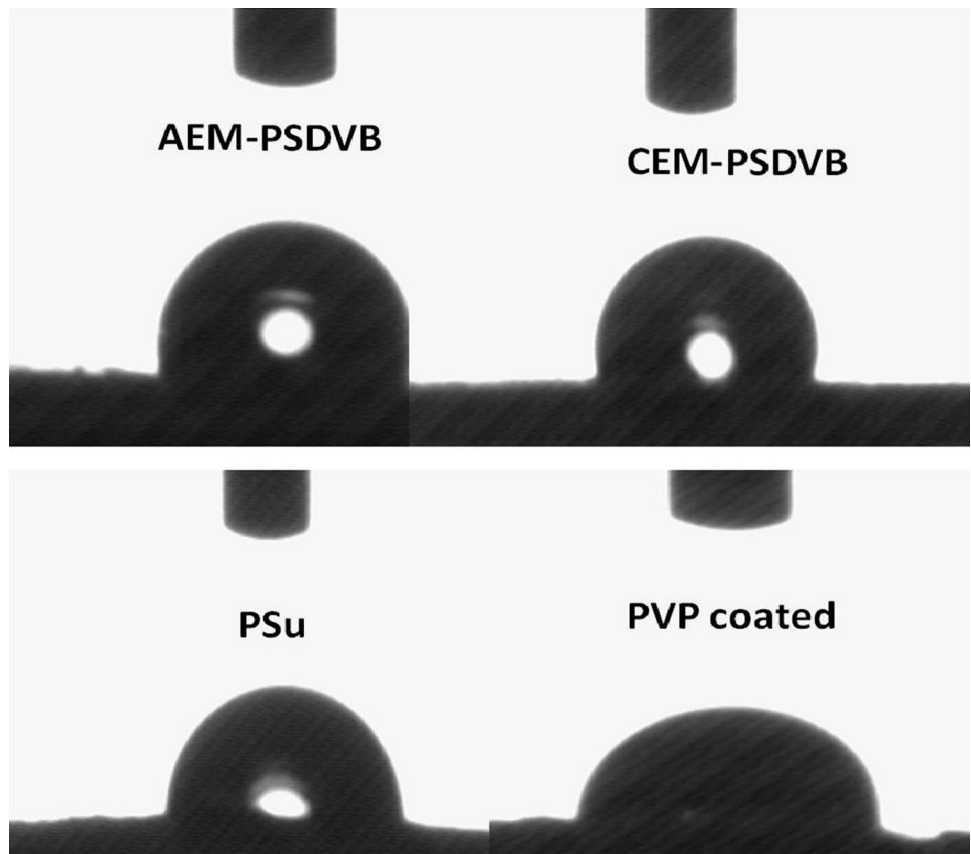


Fig. 3 SEM images of RSPSu, RQPSu, and RBPM-PVP membranes

Fig. 4 Contact angle of a water droplet on various polymeric membrane surfaces



Chemical stability

To determine the suitability of the prepared reinforced IEMs and commercial IEMs in BP MED unit, all the membranes were treated under Fenton’s reagent, so that the

peroxide which was generated attacks the polymer chain leading to a fastening of the degradation potential. Then the subjected samples were then checked for their water absorption, IEC, and conductivity values as per the standard procedures and the values are tabulated in Table 2.

Though the reinforced fiber present in the polymer chain held the ion exchange functional groups strongly, because of this enhanced degrading mechanism, the incorporated hydrophilic resin particles, and functional group that are present on the surface get leached out from the membrane due to loosening of the fiber materials upon swelling resulting in lower value when compared with its initial value (Zhu et al. 2008).

RPSu-PVP- and PSDVB-based BPM characterization

pH variation with time

Since BPM consists of RCEM and RAEM as CEL and AEL layers, respectively, which are joined together using catalytic PVP as IL, when it was placed in between the electrodes due to large electric field appearing at the membrane interface, an excess OH^- and H^+ ions were produced by the enhanced chemical reaction. This then migrated through the ion exchange layers into the distilled water-filled compartments resulting in the formation of acid and base. This principle has been depicted in Fig. 5.

Confirmation of RPSu-PVP-based membrane possessing BPM characteristics was done by analyzing the acid and base yield in the neighboring compartments as shown by changes in pH measurements. Initially the pH meter was optimized before taking readings using the distilled water. From Fig. 5 it is obvious that with increase in time, the pH of the solutions in the two compartments changed from its initial distilled water value. The compartment closer to the anode side was found to be basic in nature and the one closer to the cathode side was acidic in nature. The increasing trend in pH change with time confirmed that some ions were newly introduced only during the performance due to certain in situ reactions. And these ions were probably protons and hydroxyl ions formed on either side of the BPM by means of water splitting into its ions under the electrical driving force between the electrodes. This

conclusion was arrived at ease since there was no possibility of any other ions being present by chance since only distilled water was taken in both the compartments. On comparing RPSu-PVP-based BPM with that of commercial PSDVB-based BPM, from Fig. 5, it was found that RPSu-PVP-based BPM produced a more acidic solution than PSDVB-based BPM. In the case of basic solution, similar results were observed expecting that RPSu-PVP-based BPM took longer time to reach its highest base pH value than PSDVB-based BPM due to leakage of ions in the initial stage to the neighboring compartment.

Concentration changes with time

In the case of acid and base concentration as per Fig. 6, both RPSu-PVP- and PSDVB-based BPMs required lesser time to attain maximum acid concentration of about 0.004 N than to attain same base concentrations as revealed in pH change. Additionally, between the two BPMs, RPSu-PVP-based BPM took less time to attain maximum concentrations for both acid and base when compared to PSDVB-based BPM. In both BPMs, once the higher concentration was reached in both AC and BC; decrease in concentration was observed for BPM which exhibited a higher leakage capacity and was observed to get leveled off without further rise or decrease if the leakage was not much favored in BPM. Hence, from the above discussion and Fig. 6, it was confirmed that RPSu-PVP-based BPM showed a better BPM performance than PSDVB-based BPM. Although both BPMs showed the concentration leveling finally, after attaining its maximum in both the compartments, the difference in time taken to reach the maximum acid and base concentration was considered for this inference. In the case of RPSu-PVP-based BPM, through a steady increase in concentration, highest acid and base concentration was finally attained at 1 and 1½ h, respectively, while for PSDVB-based BPM, it was 2 and 4 h, respectively. Additionally, it should be noted that the increase in concentration was also not regular during the

Table 2 Chemical stability test for the prepared membranes

Membrane code	IEC (meq g ⁻¹)		Water absorption (%)		Conductivity (10 ⁻³ S cm ⁻¹)	
	Initial	Final	Initial	Final	Initial	Final
RPSu	4.75	4.53	15.4	14.3	5.86	5.19
RQPSu	4.35	4.12	11	9.9	5.28	4.86
RBPM-PVP	–	–	28	26.7	7.14	6.92
CEM-PSDVB	1.6	1.5	6.5	5.4	4.86	4.64
AEM-PSDVB	1.3	1.2	3.7	3.1	4.68	4.27
BPM-PSDVB	–	–	9	8.2	4.75	4.4

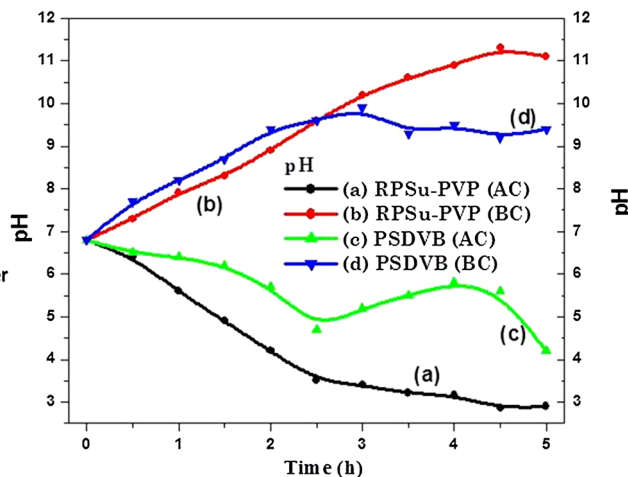
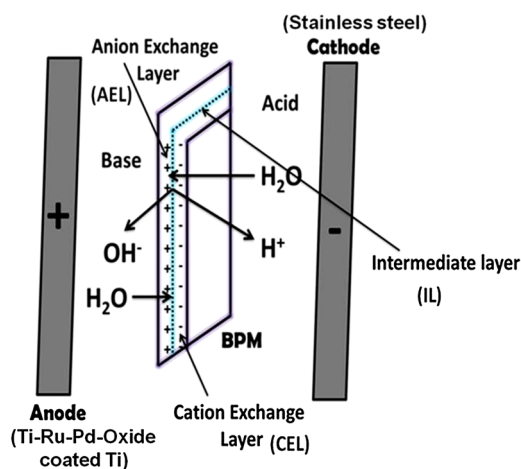


Fig. 5 Principle of BPM and Variation of pH with time in both compartments

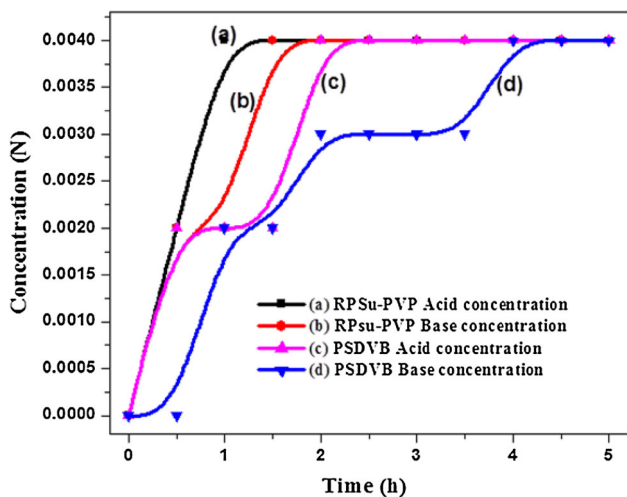


Fig. 6 Concentration change in both AC and BC with time

performance due to the leakage of ions for PSDVB-based BPM.

Current–voltage relationship

From Fig. 7, it is clear that no rectification was observed since the current was found under the applied voltage. However, the increase in current with increasing voltage proved the occurrence of water splitting in both the BPMs (Tanioka et al. 1999). On comparing the potential applied during the performance for both BPMs, RPSu-PVP-based BPM showed a higher value of up to 13.3 V than PSDVB-based BPM (11 V) for the same duration while the increase in current was observed to be lower in RPSu-PVP-based

BPM (maximum of about 47 mA) than PSDVB-based BPM (maximum of about 52 mA). Figure 7a, b represents the typical steady state I–V curve as reported by Kumar and Shahi (2010). In Fig. 7a, the variation in current due to ionic transportation was smaller when compared with Fig. 7b. This magnitude is a measure of BPM selectivity toward co-ion leakage, and may be used to predict its efficiency as per Aritomi et al. (1996). Hence, it could be concluded that RPSu-PVP-based BPM was expected to have better process efficiency due to lower co-ion leakage capacity when compared with PSDVB-based BPM. Beyond this potential, water dissociation occurs and the water splitting products (OH^-/H^+) also participated in the current transport which resulted in a steep increase in current. From this region, it could be clearly understood that the onset of water dissociation reaction occurred earlier in the case of RPSu-PVP-based BPM than PSDVB-based BPM. This in turn supports the discussion on pH and acid–base concentration of both BPM systems. The only reason for all the observed results was the difference between the two BPMs i.e., the presence of the PVP-based IL along with fiber and resin reinforcements in the case of RPSu-PVP-based BPM whereas such modification was absent in the PSDVB-based BPM system. Once the IL and resin were introduced it became more hydrophilic by attracting water from the IEL to the space charge region. The BPM, without any catalyst, increased the water dissociation resistance with an increase in current, because the water dissociation rate was slower than the ion transfer rate. The above results confirmed that the introduced PVP intermediate in RPSu-PVP-based BPM functions as a water dissociation catalyst.

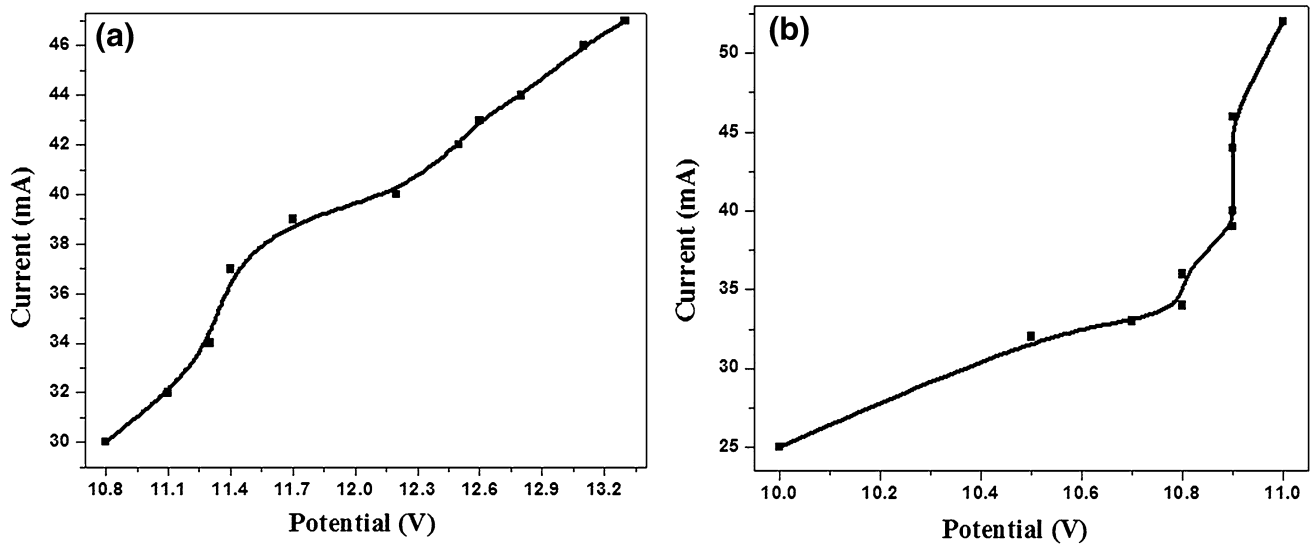


Fig. 7 Current–voltage curves for a RPSu-PVP-based BPM and b PSDVB-based BPM

BP MED performance for brine desalination

Determination of pH changes with time

Figure 8 represents the current–voltage measurement and changes of pH, acid–base production with increasing time for both RPSu-PVP and PSDVB-based IEM system. As an initial step, the pH of the solution in FC, EC, AC, and BC was observed at regular 15 min time intervals up to 8 h so as to clearly observe the mode of change of pH in these compartments. In the case of RPSu-PVP-based IEM

system, the pH in FC was observed to increase toward basicity then decrease and finally become slightly acidic in nature which was similar to the results observed by Shen et al. (2013). This is because with increasing time, higher quantities of acid were produced due to water dissociated products and thereby resulting in proton leakage through IEMs depending upon the capacity of protons to undergo back diffusion. Due to its intrinsic mobility in the presence of water, FC remained slightly acidic in nature (Xu and Yang 2002; Wang et al. 2011; Trivedi et al. 1997). On the other hand, in the case of PSDVB-based IEM system, the

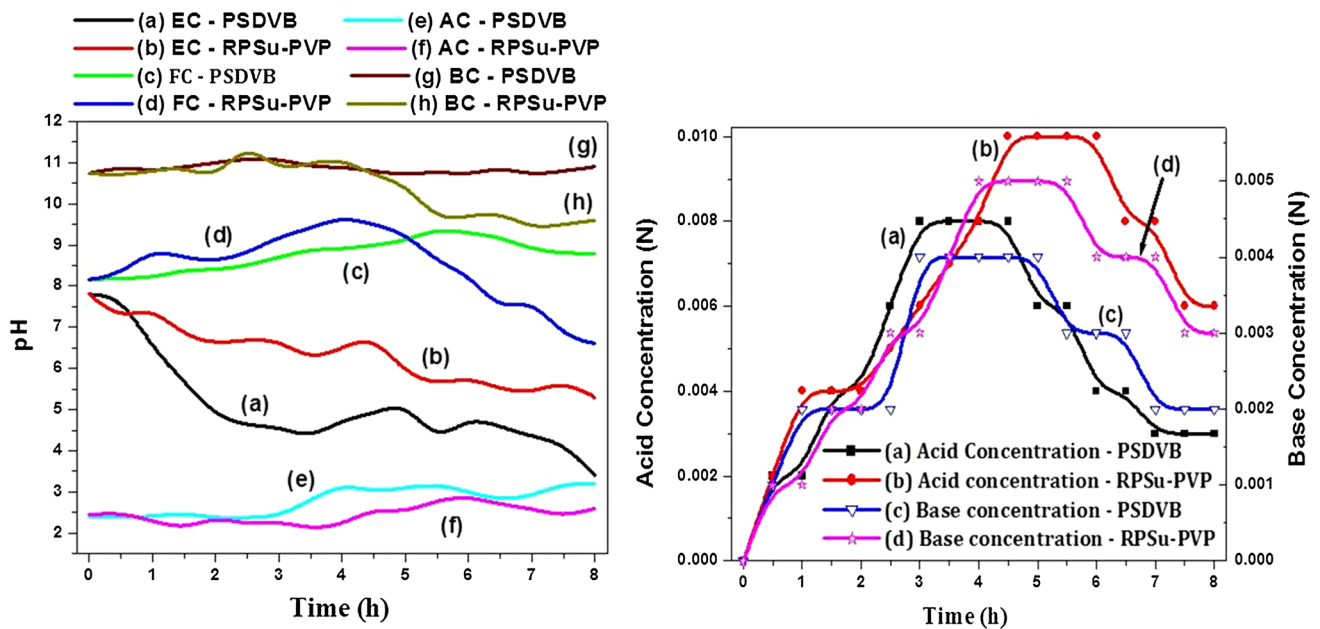


Fig. 8 Change in pH and acid–base yield with time

feed solution finally became basic in nature. The difference in pH observed between the two different systems was mainly attributed to the leakage of ions occurring through the membranes between the compartments in a stack. PSDVB-based cell experienced greater leakage of ions from BC to FC and thus it remained basic in nature. Moreover, proton leakage through IEM was low due to low concentration of acid that was produced during BPMED process using PSDVB-based IEM systems (Strathmann and Koop 2000). In the case of EC, due to the initial addition of 0.05 M NaCl solution, the pH was observed to be slightly basic in nature at their initial stages which then was observed to decrease with time. Though both the IEM systems showed the final solution to be acidic nature, the acidity was greater in the case of PSDVB-based IEM system than observed with RPSu-PVP-based IEM system. The reason for this was attributed to the higher leakage of ions through commercial membranes than that observed with synthesized membranes.

From Fig. 8, it is clear that the initial pH in AC and BC remained to be in the range of ~ 2.45 and ~ 10.74 , respectively, due to the addition of 0.01 N of acid and base solution into their respective compartments. Moreover, the pH in both AC and BC was found to rise marginally in their initial stages and was not uniform because of the leakage of certain ions into the neighboring compartments. Due to higher acid production, higher acidic pH, and greater acid leakage were observed in case of RPSu-PVP-based IEM system when compared with PSDVB-based IEM system. Whereas, in the case of basic pH, both the systems showed more or less the same pH during the first half stages of performance and later RPSu-PVP-based IEM system showed a little lower basic pH when compared with PSDVB-based IEM system. The pH change in AC and BC confirmed the acid–base production in their respective compartments which could also be confirmed by their concentration measurements. This pH variation in various compartments clearly suggested that both IEM-based systems possessed the capacity to split water into its co-ions under electric field (Shi et al. 2010; Badruzzaman et al. 2009).

Determination of acid and base concentration

When the entire ED cell was under an electric field using electrodes, the Na^+ and Cl^- ions were continuously transported from FC into BC and AC, respectively. In addition to this, due to the large electric field appearing at the membrane interface, an excess OH^- and H^+ ions produced due to the field-enhanced chemical reaction also permeate through ion exchange layers of the BPM resulting in the formation of acid and base. From the pH studies, it was evident that acid and base of certain normality

concentrations were produced in the AC and BC, respectively, while using RPSu-PVP-based IEM system and PSDVB-based IEM system in BPMED stack (Wang et al. 2012). From Fig. 8, it can be noted that acid concentration of about 0.008 N was obtained which was the maximum in AC for PSDVB-based IEM system while it was 0.01 N for RPSu-PVP-based IEM system. Whereas, the maximum base concentration in BC was observed to be 0.004 N for PSDVB-based IEM system while it was 0.005 N for RPSu-PVP-based IEM system during a brine desalination performance in BPMED.

PSDVB-based IEM cell is meant for base production rather than acid production because of higher specific permselectivity of CEM for H^+ ions as reported in the literature (Shen et al. 2013). However, from Fig. 8, the alkalinity concentration was observed to be lower in case of PSDVB-based IEM system. Furthermore, H^+ ions in the presence of water have a higher intrinsic mobility than OH^- ions and thereby resulting in more leakage of H^+ ions through commercial AEM. The T. No. of protons through AEM increased with the produced acid concentration which would also lead to their low concentration in AC (Liu et al. 2013). The maximum concentration remained constant until certain duration of time after which it decreased with increase in processing time for both types of IEM system. This suggested that the mass transfer of Na^+ and Cl^- ions through the IEM diminished due to the decrease of NaCl concentration in the feed solution. Together with the increase of the concentration of Na^+ and Cl^- ions in BC and AC, the molecular back diffusion through IEM caused by the high concentration gradient might hinder the transport of Na^+ and Cl^- ions. Furthermore, the dissociation of water molecules was also enhanced due to the Second Wien effect.

Current–voltage measurement

From Fig. 9, the current and voltage were observed to be directly proportional to each other, thereby proving that water was split at the BPM junction of RPSu-PVP-based IEM system. Also, in order to avoid high resistance, the membrane thickness used to be as thin as possible (Blaster et al. 2010). For RPSu-PVP and PSDVB-based IEM system the maximum potential points observed were 11.8 and 22.5 V, respectively, while the maximum current values observed for the same were 57 and 89 mA, respectively. The observed low voltage for RPSu-PVP-based IEM system could be explained theoretically using protonation and de-protonation reaction model and the hydrophilicity change in the interface (Fu et al. 2003). The presence of hydrogen bonding and polar interactions between the intermediate PVP and water molecules speeds up the water dissociation into hydrogen and hydroxyl ions. Thus, the

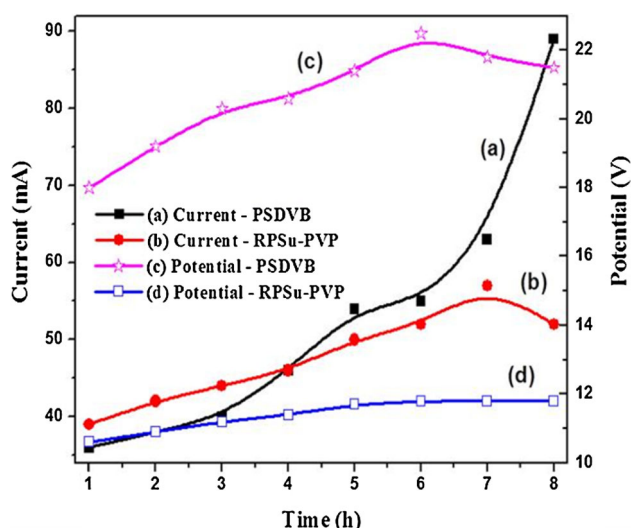


Fig. 9 Change in current and potential with time

voltage across the membrane falls and the potential decreases. On the other hand, PVP is a kind of strong hydrophilic substance and when used as an intermediate the number of hydrophilic sites in the interfacial region increased due to the high absorption of PVP which in turn increased the efficiency of water splitting.

In case of current variation with time, it was observed to increase with time for both RPSu-PVP and PSDVB-based IEM systems as shown in Fig. 9 because of the production of OH^-/H^+ during water dissociation. In other words, at the beginning of the experiments, AC and BC initially have distilled water with very low concentrations of acid and alkali. So the resistances offered by these compartments were very high as compared to the resistance offered by FC. As time passes, the concentrations of AC and BC increased because of the continuous formation of acid and alkali in these compartments and all the solutions were being continuously recycled. Hence, the resistance of these compartments was decreased. On the other hand, the concentration of salt in FC decreased due to the continuous transport of ions from these compartments. As a result, the resistance of these compartments increased. The net effect was the overall decrease in stack resistance with time, resulting in an increase in current production with time. But in the case of RPSu-PVP-based system, unlike that of the PSDVB-based system, the final current was slightly lower due to the concentration polarization phenomenon and difference in membrane resistance in the stack. The maximum current observed for both RPSu-PVP and PSDVB-based IEM systems was about 57 and 89 mA, respectively.

In the case of voltage versus time curve, the curve which was inclined to be a line in parallel to the X-axis for both the cases, indicated that PSDVB and RPSu-PVP-based

system were chemically stable when it was used for water dissociation as described by Xue et al. (2006). The purity of acid and alkali increased with an increase in voltage to some extent, after which further increase in voltage had an adverse effect on membranes, concentration, and purity of acids and bases depending upon the current rate of water dissociation on the IL surface of BPM as well as the rate of ion transport through the monopolar membranes. This was mainly because it causes heating of stack and deterioration of membrane properties as discussed by Trivedi et al. (1997).

Determination of WDE, T. No. of ions, and fluxes

The efficiency of BPMED is strongly affected by the transport properties of ions present in the solution through various functionalized IEMs. WDE is one of the most important parameters for determining the process efficiency, which was closely related to the membrane's transport properties. Under an electric field, at the beginning of the BPMED process, there was a competition between these ions for transport, and the transfer of a large amount of Na^+ and Cl^- ions through the IEM resulted in a slow transfer of H^+ and OH^- ions. This was because of the maximum availability of initial salt concentration in FC when compared with the water-dissociated ions. As the operation time passed, the dissociation of large amounts of water molecules resulted in the large accumulation of H^+ and OH^- . It should be noted that once all the Na^+ and Cl^- ions were transported from the FC, the accumulated H^+ and OH^- were also transported very efficiently resulting in the higher WDE after the first half performance time. This also explained the reason for the observed higher T. No. of ions with time during the first half part of the performance and a decrease in its value during the later stages of performance for the same membrane (Shen et al. 2013).

Ion transport number is a quantity which is indicative of the different contributions of ions to the electric current in electrolytes due to their varied electrical mobility. Since CE depends upon the ion transport and ionic mobility of an ion for a better process efficiency it was expected that the system should have higher T. No. of ion. Figure 10 represents the T. No. properties of both sodium and chloride ions for RPSu-PVP-based and PSDVB-based IEM system, respectively. From Fig. 10 it is clear that T. No. of both Na^+ ion and Cl^- ions decreased with increase in time for both the IEM systems. This was because NaCl concentration that was available for migration started to decrease with increase in time as discussed above. However, the performance was running steadily, mainly because the current was carried by the water dissociated products such as H^+ and OH^- ions. Depending upon the membrane capacity the higher T. No. was observed to be its initial

value. In both IEM systems, the chloride ion T. No. was observed to be greater than sodium ion T. No. value as reported in literature. The initially observed results for T. No. of sodium and chloride ion, i.e., 0.11 and 0.33 values decreased to 0.04 and 0.08, respectively, for RPSu-PVP-based system while in case of a PSDVB-based system, T. No. of sodium and chloride ion decreased from its initial of about 0.4 and 0.5 to 0.37 and 0.42, respectively, in brine desalination performance.

Based upon the feed concentration, pH variations in AC and BC during the stack performance, time, and membrane capacity, the occurrence of water dissociation on BPM interface was confirmed. From Fig. 11, it is clear that WDE increased with increase in time. The reason for this variation of WDE with time is the same as discussed for T. No. of ions. The higher WDE of about 0.88 was obtained for RPSu-PVP and it was 0.21 for PSDVB-based IEM system. The highest T. No. and steady increase in WDE with time observed for RPSu-PVP-based IEM system was mainly due to the increase in electric field, pre-polarization of water molecules at the membrane-solution interface, and the presence of a hydrophilic catalytic PVP intermediate in between the two monopolar layers of BPM. According to Ren et al. (2008), the reduction in the ionic transport rate during later stages of the performance was often correlated with an increased membrane resistance due to the presence of a mixture of organic matter and inorganic salts. As a consequence, during the performance of brine desalination, slight membrane fouling was observed for both RPSu-PVP-based and PSDVB-based IEM systems. It is also noted from Fig. 11 that in both cases, whether acidic or basic, the water dissociation fluxes decreased with time.

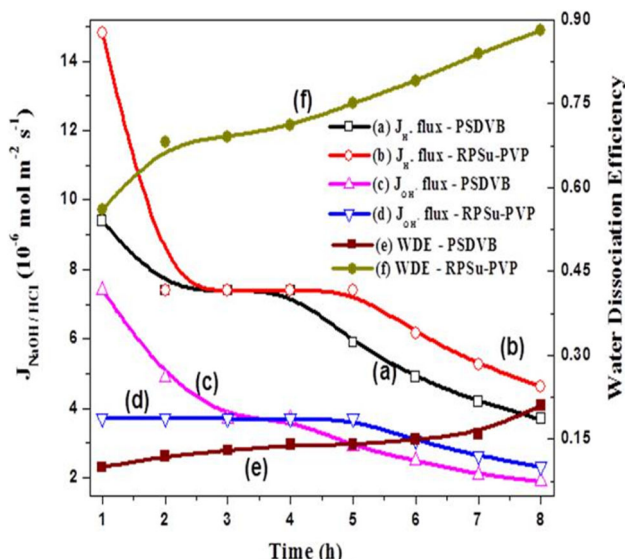


Fig. 10 Change in T. No. properties of both sodium and chloride ions with time

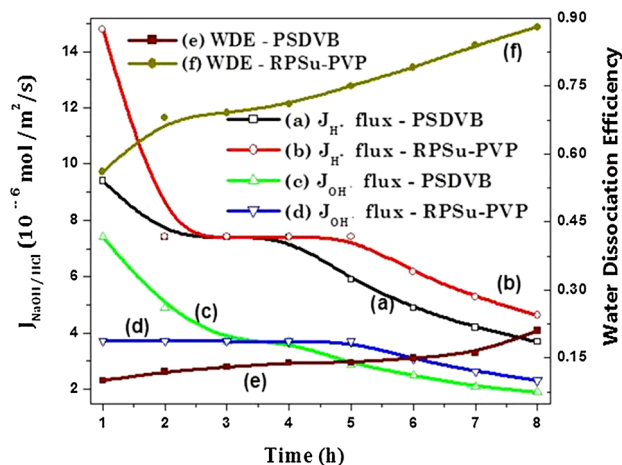


Fig. 11 Change in WDE and water dissociation fluxes of both proton and hydroxyl ion with time

The main reason for the decrease in acid and base flux was due to the depletion of Na^+ in anode compartment and Cl^- ion in cathode compartment and the availability of NaCl in FC for the conversion into the acid and base. Higher acidic and basic fluxes were observed to be 9.4×10^{-6} and $7.4 \times 10^{-6} \text{ mol m}^{-2} \text{ s}^{-1}$ for PSDVB-based system and 14.8×10^{-6} and $3.71 \times 10^{-6} \text{ mol m}^{-2} \text{ s}^{-1}$ for RPSu-PVP-based systems, respectively.

Determination of process efficiency parameters

For any system, higher CE with lower energy consumption is one of the factors which determine the feasibility of electrochemical process toward higher process efficiency. It is clear from Fig. 12 that CE of BPMED stack decreased with operation time for both types of IEM systems. This can be explained by invoking the concept of ion leakage through IEM as discussed in the case of T. No. of ions. CE was observed to decrease from 38 % with time for the PSDVB-based system while it was 45 % for RPSu-PVP-based system. On the other hand, in the case of energy consumption, it increased with an increase in time as per shown in Fig. 12. The increase in the energy consumption was mainly attributed to the fact that a large part of the total electrical energy was consumed to overcome the electrical resistance. The applied voltage declined sharply at the start of the BPMED procedure. This was mainly related to either the increase in conductivity of the HCl/NaOH solution in AC/BC or caused due to the exhaustion of NaCl in the feed solution. The increase in resistance of FC, resulted from the exhaustion of NaCl in the solution, can be offset by a decrease in the electrical resistance of AC and BC caused by an increase in the HCl and NaOH concentrations as a consequence of transfer of Cl^- and Na^+ ions from the feed solution. Since the transformation of

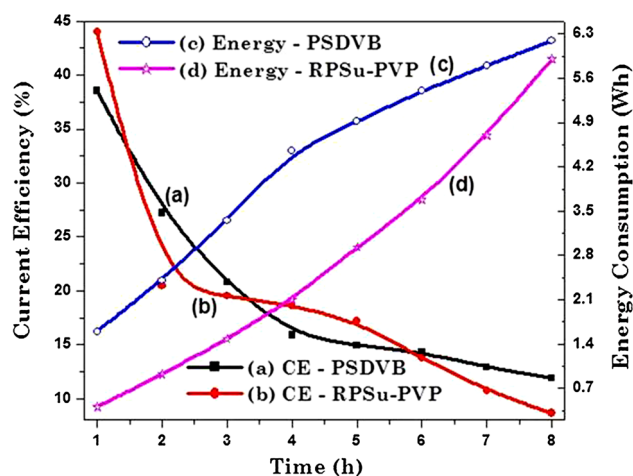


Fig. 12 Change in CE and energy consumption with time

NaCl into an acid and base solution was fully realized, the electrical resistance of feed solution increased, resulting in a sharp increase in the voltage drop. Thus, the energy consumption was observed to increase with time and reached a maximum of 6.2 Wh for PSDVB-based system and 5.9 Wh for RPSu-PVP-based system.

Determination of electrical conductivity, salinity, and sodium-chloride ion concentration

To evaluate the purity of the generated acid and base during the performance and to confirm the capacity of both synthesized and commercial BPM regarding their efficiency to dissociate water into its ions, certain important parameters such as electrical conductivity, salinity, sodium ion, and chloride ion concentrations were analyzed. Table 3 represents the electrical conductivity, salinity, and sodium-chloride ion concentration values in 100 ml of feed sample solutions for both RPSu-PVP and PSDVB-based IEM systems, respectively. Though the removal of NaCl ions from the FC was confirmed by its electrical conductivity measurements; the effectiveness of this process was confirmed by its salinity measurements. The observance of lower salinity and electrical conductivity than its initial value was mainly because of the migration of the salt ions from the FC toward the neighboring compartment. Thus, this result suggested that the water obtained after the BPMED desalination performance was expected to have a better quality than their initial sample.

With respect to sodium and chloride ion concentration, the final feed solutions showed a lower value than its initial salt sample solution for both ion concentrations in case of the two types of IEM systems. This clearly confirmed the migration of ions under the electric field from FC to neighboring compartment. The increase in final Na⁺ and

Table 3 Electrical conductivity, salinity, and sodium-chloride ion concentration values for RPSu-PVP and PSDVB-based IEM systems

Parameters	RPSu-PVP based IEM system	PSDVB based IEM system
Electrical conductivity (mS cm ⁻¹)		
Initial	17.17	17.17
Final	7.0	12.02
Salinity (%)		
Initial	11.5	11.5
Final	5.1	7.9
Chloride ion concentration [mg (100 mL) ⁻¹]		
Initial	10.3	10.3
Final	6.6	8.6
Sodium ion concentration (ppm)		
Initial	9.0	9.0
Final	4.4	8.0

Cl⁻ ion concentrations with an increase in feed concentration was mainly because of two reasons. First was due to the increased NaCl concentrations in the feed solutions. The second reason was due to the restricted transport of sodium ion and chloride ion through IEMs because of decreased membrane capacity, which was due to the adhesion of the salt ions over the surface of the membrane which in turn was mainly because of the longer duration of previous performances. The higher the difference between the initial and final value effective was the process in the removal of NaCl and higher acid–base concentration with higher purity.

Conclusions

A novel resin-glass fiber-reinforced functionalized PSu-based IEMs were prepared and characterized using FTIR, TGA, SEM, and contact angle measurements. The chemical stability of the prepared IEMs was determined by means of ionic conductivity, water absorption, and IEC. The BPM efficiency of prepared RPSu-PVP and PSDVB-based IEM systems were evaluated using pH and concentration measurements. Brine desalination performance results obtained for various parameters using RPSu-PVP-based IEM system were compared with PSDVB-based IEM system. Based on the results obtained for various process parameters such as CE (maximum of about 45 % for RPSu-PVP and 38 % for PSDVB), energy consumption (of about 0.41 Wh for RPSu-PVP and 1.60 Wh for PSDVB), acid–base production (maximum of about 0.010 N acid: 0.005 N base for RPSu-PVP and 0.008 N acid: 0.004 N base for PSDVB), and WDE (maximum as

0.88 for RPSu-PVP and 0.21 for PSDVB), it was concluded that RPSu-PVP-based IEM system showed a better performance than that of the commercial PSDVB-based IEM system. In addition, electrical conductivity, salinity, and sodium-chloride ion concentration results were obtained for both types of IEM systems and compared.

Acknowledgments Financial support from the Board of Research in Nuclear Science (BRNS), Mumbai, India (Letter No. 2010/37C/1/BRNS/826, Dated: 28–06–2010) is gratefully acknowledged. The authors thank for Goniometer facility help in Polymer Engineering and Colloids Science Laboratory, Chemical Engineering Department, IIT Madras.

Open Access This article is distributed under the terms of the Creative Commons Attribution 4.0 International License (<http://creativecommons.org/licenses/by/4.0/>), which permits unrestricted use, distribution, and reproduction in any medium, provided you give appropriate credit to the original author(s) and the source, provide a link to the Creative Commons license, and indicate if changes were made.

References

- Aritomi T, van der Boomgaard T, Strathmann H (1996) Current voltage curve of a bipolar membrane at high current density. *Desalination* 104:13–18
- Badruzzaman M, Oppenheimer J, Adham S, Kumar M (2009) Innovative beneficial reuse of reverse osmosis concentrate using bipolar membrane electro dialysis and electrochlorination processes. *J Membr Sci* 326:392–399
- Blaster J, Srinkantharajah S, Sumbharaju R, Pünt I, Lammertink RGH, Stamatialis DF, Wessling M (2010) Tailoring the interface layer of the bipolar membrane. *J Membr Sci* 365:389–398
- Dias CR, de Pinho MN (1999) water structure and selective permeation of cellulose based membranes. *J Mol Liquids* 80:117–132
- Friette VJ (1956) Preparation and characterization of bipolar ion-exchange membranes. *J Phys Chem* 60:435–439
- Fu RQ, Xu TW, Wang G, Yang WH, Pan ZX (2003) PEG - catalytic water splitting in the interface of a bipolar membrane. *J Colloid Interface Sci* 263:386–390
- Guan R, Zou H, Lu D, Gong C, Liu Y (2005) Polyethersulfone sulfonated by chlorosulfonic acid and its membrane characteristics. *Eur Polym J* 41:1554–1560
- Kressman TRE, Tye FL (1956) The effect of current density on the transport of ions through ion-selective membranes. *Discuss Faraday Soc* 21:185–292
- Krishnaveni V, Sangeetha D (2012) Desalination efficiency of a novel bipolar membrane based on functionalized polysulfone. *Desalination* 296:37–45
- Krishnaveni V, Sangeetha D (2014a) Investigation on the application of polysulfone based bipolar membrane for desalination of water. *Desalin Water Treat*. doi:10.1080/19443994.2014.881751
- Krishnaveni V, Sangeetha D (2014b) Evaluation of synthetic salt water desalination by using a functionalized polysulfone based bipolar membrane electro dialysis cell. *Desalination* 344:189–197
- Krishnaveni V, Sangeetha D (2015) Evaluation of efficiency of brackish desalination ion exchange membranes using electro dialysis process. *RSC Adv* 5:73901–73913
- Kumar M, Shahi VK (2010) Heterogeneous–homogeneous composite bipolar membrane for the conversion of salt of homologous carboxylates into their corresponding acids and bases. *J Membr Sci* 349:130–137
- Liu Z, Zhu M, Yu P, Xu Y, Zhao X (2013) Pretreatment of membrane separation of glyphosate mother liquor using a precipitation method. *Desalination* 313:140–144
- Ostwald W (1890) Elektrische eigenschaften halbdurchlässiger scheidewände. *Z Phys Chem* 6:71
- Ren H, Wang Q, Zhang X, Kang R, Shi S, Cong W (2008) Membrane fouling caused by amino acid and calcium during bipolar membrane electro dialysis. *J Chem Technol Biotechnol* 83:1551–1557
- Sachdeva S, Ram RP, Singh JK, Kumar A (2008) Synthesis of anion exchange polystyrene membranes for the electrolysis of sodium chloride. *AIChE J* 54:940–949
- Shen J, Huang J, Liu L, Ye W, Lin J, Bruggen BV (2013) The use of BMED for glyphosate recovery from glyphosate neutralization liquor in view of zero discharge. *J Hazard Mater* 260:660–667
- Shi S, Lee YH, Yun SH, Phan V, Hung X, Moon SH (2010) Comparisons of fish meat extract desalination by electro dialysis using different configurations of membrane stack. *J Food Eng* 101:417–423
- Strathmann H, Koop GH (2000) Process economics of the electro-dialytic water dissociation for the production of acid and base. In: Kemperman AJB (ed) *Handbook on bipolar membrane technology*. Twente University Press, Enschede, pp 193–218
- Tanioka A, Shimizu K, Hosono T, Eto R, Osaki T (1999) Effect of interfacial state in bipolar membrane on rectification and water splitting. *Colloids Surf A* 159:395–404
- Trivedi GS, Shah BG, Adhikary SK, Indusekhar VK, Rangarajan R (1997) Studies on bipolar membranes, part II. Conversion of sodium acetate to acetic and sodium hydroxide. *React Funct Polym* 32:209–215
- Ulbricht M (2006) Advanced functional polymer membranes. *Polymer* 47:2217–2262
- Volkov VV, Mchedlishvili BV, Roldugin VI, Ivanchev SS, Yaroslavlsev AB (2008) Membranes and nanotechnologies. *Nanotechnol Russia* 3:656–687
- Wang Y, Zhang X, Huang C, Xu T (2011) Production of monoprotic, diprotic, and triprotic organic acids by using electro dialysis with bipolar membranes: effect of cell configurations. *J Membr Sci* 385:226–233
- Wang X, Wang Y, Zhang X, Xu T (2012) In situ combination of fermentation and electro dialysis with bipolar membranes for the production of lactic acid: operational compatibility and uniformity. *Bioresour Technol* 125:165–171
- Xu T, Yang W (2002) Effect of cell configurations on the performance of citric acid production by a bipolar membrane electro dialysis. *J Membr Sci* 224:1
- Xue YH, Fu RQ, Fu YX, Xu TW (2006) Fundamental studies on the intermediate layer of a bipolar membrane V. Effect of silver halide and its dope in gelatin on water dissociation at the interface of a bipolar membrane. *J Colloid Interface Sci* 298:313–320
- Zhu X, Liang Y, Pan H, Jian X, Zhang Y (2008) Synthesis and properties of novel H-bonded composite membranes from sulfonated poly (phthalazinone ether)s for PEMFC. *J Membr Sci* 312:59–65